# A thermionic energy converter with a molybdenum-alumina cermet emitter

# A thermionic energy converter with a molybdenum-alumina cermet emitter

G. H. M. Gubbels, L. R. Wolff, and R. Metselaar
*Centre for Technical Ceramics, Eindhoven University of Technology, P. O. Box 513, 5600 MB Eindhoven, The Netherlands*

(Received 13 June 1990; accepted for publication 2 July 1990)

A study is made of the properties of cermets as electrode materials for thermionic energy converters. For thermodynamic reasons it is expected that all cermets composed of pure Mo and refractory oxides have the same bare work function. From data on the work function of Mo in an oxygen atmosphere this bare work function is estimated to be $\Phi = 4.9$ eV (at $T = 1400$ °C). Experimentally, the bare work function of $Al_2O_3$-Mo cermets was found to be $\Phi = 4.5$ eV, independent of the relative amounts of $Al_2O_3$ and Mo. The cesiated work function of the $Al_2O_3$-Mo cermets was found to be 0.15 eV lower than the cesiated work function of pure Mo. The bare work function of $Mo_3Al$ was found to be $\Phi = 4.0$ eV. The cesiated work function of $Mo_3Al$ at collector temperature conditions was 0.3 eV lower than the cesiated work function of pure Mo. The electrical power density of a diode with an $Al_2O_3$-Mo cermet emitter was 0.4 W/cm$^2$ at 1300 °C. The barrier index at this temperature was 2.36 V. The high barrier index is attributed to a high plasma voltage drop $V_d = 0.91$ V.

## I. INTRODUCTION

A thermionic energy converter (TEC) is a device which directly converts heat into electricity. It consists of two electrodes, one of which (the emitter) is heated to a temperature at which it will thermally emit electrons. The other electrode (the collector) is kept at a lower temperature and collects the electrons. Part of the energy, removed from the emitter by evaporating electrons and transported to the collector, is transformed into heat by condensing electrons. The remaining part is converted into electrical power in the load as the electrons return to emitter potential. Details about the principles of operation and examples of applications have been described elsewhere.[1–3]

In order to facilitate the commercial application of combustion heated TECs, higher efficiency and lower material costs are required. For the realization of a higher efficiency, Henne[4] suggested the use of a mixture of a ceramic and a metal as an emitter: an $UO_2$-Mo cermet emitter. Henne found an electrical power density of 5 W/cm$^2$ at 1350 °C. This is one of the highest electrical power densities ever obtained in a TEC at such a rather low emitter temperature. The electrical power density is about two times higher than in TECs with the usual Mo electrodes.[1,5] Henne estimates the efficiency ($\eta$) of the diode with the Mo-$UO_2$ cermet emitter to be 15%.[4] The maximal obtainable efficiency, i.e., the Carnot efficiency, is about 50%. To reach this value is a great engineering challenge. One way to get closer to the Carnot efficiency may be to use improved electrode materials.

From the published current-voltage ($I$-$V$) characteristics of a diode with a Mo-$UO_2$ emitter,[4] we deduce a work function of $\Phi_e = 2.35$ eV for a cesiated $UO_2$-Mo emitter at a reduced emitter temperature of $T_e/T_{Cs} = 3.23$. The reduced emitter temperature is defined as the emitter temperature ($T_e$) divided by the cesium reservoir temperature ($T_{Cs}$), both in K. The cesiated emitter work function of the Mo-$UO_2$ emitter is about 0.5 eV lower than the value for pure polycrystalline molybdenum.[6] As a result, the optimum cesium reservoir temperature is low (230 vs 310 °C), resulting in a low plasma voltage drop. Henne also found low values for the cesiated collector work functions ($\Phi_c = 1.2$–$1.3$ eV).[4] However, these values are not very reliable, because no guard rings were used in his diode. Henne attributed the low cesiated collector work function to the evaporation of electronegative substances which improved the collector properties.

In order to investigate whether the high efficiency of a cermet electrode is only the result of the presence of oxygen or whether the accompanying element also has an effect, we decided to investigate a cermet different from Mo-$UO_2$. Mo-$Al_2O_3$ was chosen as a cermet emitter material, because of the assumed compatibility of molybdenum and alumina and because of the high stability and high melting temperature of alumina (2045 °C). In the present research diode the $Al_2O_3$-Mo cermet emitter faces a polycrystalline Mo collector.

In Sec. II we will present a thermodynamic analysis of the Mo-Al-O and the Mo-U-O system. The oxygen partial pressure above the various cermet emitters at the emitter temperature will be calculated. In Sec. III the manufacture and morphology of these $Al_2O_3$-Mo cermet emitters will be described. The molybdenum collector surface facing the cermet emitter was characterized too. The research diode will be described in Sec. IV. The measurement of the bare and cesiated work function is illustrated in Sec. V. Ignited mode $I$-$V$ characteristics of the diode equipped with a Mo-$Al_2O_3$ emitter are presented in Sec. VI. In the final section the various cermet emitters are compared with each other and with the commonly used refractory metal electrodes.

## II. PHASE DIAGRAM AND PARTIAL PRESSURES

An isothermal section ($T = 1400$ °C) of the phase diagram of the Mo-Al-O system is presented in Fig. 1. The phase equilibria in the three boundary binary systems are

 0021-8979/90/235856-10$02.40  

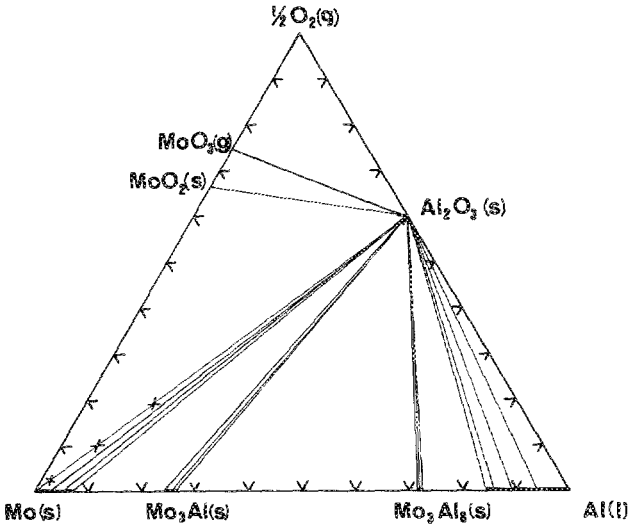


FIG. 1. Isothermal section of the calculated phase diagram of the Mo-Al-O system at a temperature of 1400 °C and a pressure of 1 bar. The overall concentrations of the cermets used in our experiments are indicated with crosses (x).

taken from the literature.[7] The equilibria in the ternary system are calculated from the Gibbs energies of formation of the various compounds at the fixed temperature (1400 °C). The Gibbs energies of formation are the reaction Gibbs energies at standard conditions ($\Delta G^\circ$) of the reaction:

$$\mathrm{Mo}(s) + \mathrm{O}_2(g) \rightarrow \mathrm{MoO}_2(s) \quad (1)$$

$$2\mathrm{Al}(l) + 3/2\mathrm{O}_2(g) \rightarrow \mathrm{Al}_2\mathrm{O}_3(s) \quad (2)$$

$$\mathrm{Al}(l) + 3\mathrm{Mo}(s) \rightarrow \mathrm{Mo}_3\mathrm{Al}_8(s) \quad (3)$$

$$8\mathrm{Al}(l) + 3\mathrm{Mo}(s) \rightarrow \mathrm{Mo}_3\mathrm{Al}_8(s). \quad (4)$$

Standard conditions chosen here are: the condensed phases are in a pure state and the gases in the reaction equation have a partial pressure of 1 atm. Values of the $\Delta G^\circ$ of the reactions (1) and (2) were taken from handbooks.[8] Values for the reactions (3) and (4) were deduced from the investigations of Shilo *et al.*[9] As an example, if one wants to know whether $MoO_2$ and $Mo_3Al$ are in mutual equilibrium or Mo and $Al_2O_3$, the reaction:

$$4\mathrm{Mo}_3\mathrm{Al}(s) + 3\mathrm{MoO}_2(s) \rightarrow 15\mathrm{Mo}(s) + 2\mathrm{Al}_2\mathrm{O}_3(s) \quad (5)$$

is considered. Using a suitable combination of reactions (1), (2) and (3) [i.e., 2*Eq. (2)-4*Eq. (3)-3*Eq. (1)], $\Delta G^\circ$ of reaction (5) can be calculated. It is found that $\Delta G^\circ$ of reaction (5) is negative, so Mo and $Al_2O_3$ are in mutual equilibrium at the given temperature. The corresponding tie line is drawn in the isothermal section of the phase diagram (see Fig. 1). All possible equilibria were studied this way. The isothermal section presented in Fig. 1 is the result of this study.

We prepared the cermet by sintering pure Mo and $Al_2O_3$ in vacuum. Thus the overall concentration at the start of the sintering process lies on the boundary tie line of the two-phase regions $Mo/Al_2O_3$ and the three-phase region $Mo/MoO_2/Al_2O_3$. As the amount of oxygen on the electrode surface is assumed to be of importance,[1] we will calculate the oxygen partial pressure ($p_{O_2}$) in equilibrium with $Al_2O_3$-Mo mixtures at 1400 °C. The oxygen pressure above $Al_2O_3$ and pure Mo will be the oxygen pressure corresponding to the three-phase region $Mo/Al_2O_3/MoO_2$. This oxygen partial pressure is governed by reaction Eq. (1). From the Gibbs energy of this reaction at standard conditions the oxygen partial pressure can be estimated by using the equation:

$$\Delta G^\circ = RT \ln(p_{O_2}), \quad (6)$$

where $T$ is the temperature in K, and $R$ is the gas constant. The oxygen partial pressure at 1400 °C is found to be $p_{O_2} = 2\times10^{-7}$ mbar. In a same way the partial pressures of the other gases can be calculated from the thermodynamic data.[10] The calculated partial pressures of the most volatile molecules are presented in Table I.

TABLE I. Calculated partial pressure ($p$ in mbar) of various molecules at 1400 °C in three phase regions in the Mo-Al-O system.

| | $O_2/MoO_2/Al_2O_3$ | $Mo/MoO_2/Al_2O_3$ | $Mo/Al_2O_3/Mo_3Al$ |
|---|---|---|---|
| $P_{O_2}$ | $4\times10^{-3}$ | $2\times10^{-7}$ | $2\times10^{-13}$ |
| $p_{MoO_3}$ | $1\times10^{+3}$ | $4\times10^{-4}$ | $4\times10^{-13}$ |
| $p_{MoO_2}$ | $6\times10^{+1}$ | $3\times10^{-8}$ | $2\times10^{-35}$ |
| $p_{Mo}$ | $3\times10^{-20}$ | $1\times10^{-9}$ | $9\times10^{-10}$ |
| $p_{Al2O}$ | $8\times10^{-28}$ | $1\times10^{-14}$ | $2\times10^{-8}$ |
| $p_{AlO}$ | $5\times10^{-13}$ | $1\times10^{-10}$ | $5\times10^{-9}$ |
| $p_{Al}$ | $2\times10^{-15}$ | $3\times10^{-7}$ | $1\times10^{-3}$ |

During the outgasing procedure of the diode the total pressure in the diode is lower than $10^{-7}$ mbar. At the start of the outgasing procedure, the surface of the cermet emitter will be a little oxidized. So the overall composition of the cermet will lie in the three-phase region $Mo/Al_2O_3/MoO_2$ near the $Al_2O_3$/pure Mo tie line. The partial pressures in the interelectrode space of the diode will correspond to the partial pressures in the three phase region $Mo/Al_2O_3/MoO_2$. The Mo matrix will be saturated by oxygen. Values of the oxygen solubility in the Mo matrix are given in the literature.[11,12] However, the uncertainty is high. The values range from $c_O = 0.0008$ to $c_O = 0.04$ at.% at 1400 °C. It is seen from Table I that the $MoO_3$ pressure is the highest pressure. Due to the evaporation of $MoO_3$ the overall composition of the $Al_2O_3$-Mo cermet will move in the phase diagram over a line connecting the $MoO_3$ composition and the starting overall composition. The $MoO_3$ is expected to condense on the collector. This evaporation process will stop when the overall composition reaches the $Al_2O_3$/pure Mo tie line. As calculated above, the partial oxygen pressure will be $2\times10^{-7}$ mbar. Greaves and Stickney[13] investigated the thermionic work function of molybdenum at high temperature and various oxygen pressures. Extrapolating these data to a oxygen partial pressure of $2\times10^{-7}$ mbar and a temperature of 1400 °C we find a work function of 4.9 eV, i.e., the oxygen occupation density $\Theta = 1$ and the maximal increase of work

function is found. As the oxygen partial pressure is independent of the relative amount of oxide and pure molybdenum, the work function will be independent of this amount too. Thus, in a perfectly outgased diode we expect a Mo-$Al_2O_3$ cermet to have a work function of 4.9 eV.

Next in the hierarchy of partial pressures is $Al(g)$ (see Table I). It is a thousand times lower than the $MoO_3$ partial pressure. As a result of the lower collector temperature, Al will be deposited on the collector. The oxygen partial pressure is about the same as the $Al(g)$ pressure. Since oxygen cannot condense at this temperature, it will be removed from the diode by the vacuum pump during the outgasing procedure. In fact, thermodynamic equilibrium will never be reached as the diode is an open system.

In the bulk of the cermet emitter we expect a slow decomposition of $Al_2O_3$ and dissolution of the constituents in Mo, according to the reactions:

$$Al_2O_3(s) \rightarrow 2Al(l) + 3/2O_2(g), \tag{7a}$$

$$2Al(l) \rightarrow 2[Al]_{Mo}, \tag{7b}$$

$$3/2O_2(g) \rightarrow 3[O]_{Mo}, \tag{7c}$$

which results in the overall reaction:

$$Al_2O_3(s) \rightarrow 2[Al]_{Mo} + 3[O]_{Mo}. \tag{7d}$$

The $\Delta G^\circ$ of this reaction (7d) is the sum of the $\Delta G^\circ$'s of the three reactions (7a), (7b), and (7c). $\Delta G^\circ$ of the overall reaction (7d) will be reduced because the heat of solution of Al in Mo is large ($\Delta H = -20$ kJ/grat),[14] i.e., $\Delta G^\circ_7(7b) = -40\,000 + 2RT\ln(x_{Al})$. Some data on the heat of solution of oxygen in molybdenum are available from literature,[12] but the uncertainty is high $\Delta G^\circ_{1673}(7c) = -63 +/- 75$ kJ. If reaction (7d) proceeds, we expect Al to be detectable in the Mo matrix after the experiment. The more Al is dissolved in the Mo matrix the lower the oxygen partial pressure at the surface of the cermet will be. A corresponding lower work function is expected to be found.

The phase diagram of the ternary Mo-U-O system is calculated too. Data of the binary U-O system were taken from Gmelin's Handbook.[15] An isothermal section at 1400 °C is presented in Fig. 2. The partial oxygen pressure at the $UO_2$-Mo emitter surface is determined by the same reaction Eq. (1) as in the case of the $Al_2O_3$-Mo cermet. Thus from these simplified thermodynamic considerations, it is concluded that the same oxygen partial pressure applies for all Mo cermet emitters. At 1400 °C it is $2\times10^{-7}$ mbar, and if it is assumed that oxygen from the oxide is the main cause of the work function change, i.e., the residual oxygen pressure in the diode is lower than the equilibrium oxygen pressure of Mo-$MoO_2$ mixtures, then all Mo-cermets are expected to have the same bare work function, i.e., $\Phi = 4.9$ eV at 1400 °C.

If the residual oxygen pressure in the diode is higher than the oxygen pressure corresponding to the three phase equilibrium, e.g., due to some oxygen source in the diode, the work function is still expected to be $\Phi = 4.9$ eV, because the maximal increase of the work function due to the presence of oxygen has already been reached.[13]

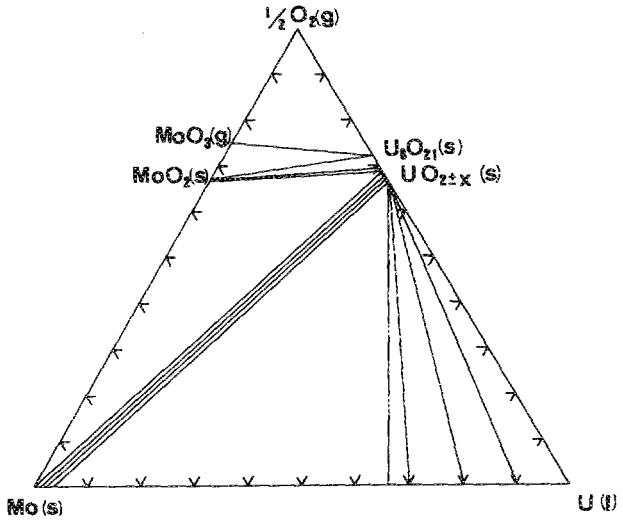


FIG. 2. Isothermal section of the calculated phase diagram of the U-Mo-O system at a temperature of 1400 °C and a pressure of 1 bar.

## III. DESCRIPTION OF THE DIODE

A sketch of the diode is shown in Fig. 3. The diode is situated in an evacuated bell jar to protect it against corrosion by air. The various parts of the diode are interconnected using stainless-steel flanges joined by copper gaskets. The guard ring and the collector are made of arc-cast polycrystalline molybdenum. The emitter substructure is made of molybdenum too. Electrical insulation of the guard ring, collector, and emitter is achieved by alumina rings connected by metal O gaskets (see Fig. 3). The interelectrode distance is variable and adjustable in the range from 0.01 to 2.0 mm, even during operation. During the experiments, the emitter, collector, and cesium reservoir temperatures were automatically controlled and measured with Pt-Pt/Rh thermoelements. The emitter temperature was constant within 5 °C, the collector temperature within 1 °C, and the cesium reservoir temperature also within 1 °C. In order to reach a sufficiently high emitter temperature (up to 1500 °C) a 0.5-mm-diam tungsten 26% rhenium filament was used in the electron gun. The bell jar protecting the diode is evacuated by an oil diffusion pump. The diode is evacuated by a separate pumping system using a turbomolecular pump and for the ultimate vacuum an AEI triode ion pump (120 l/s). Before the diode is assembled, all parts are thoroughly cleaned with freon, ethanol, and distilled water. The diode was outgased at temperatures as high as the highest temperatures to be used in the experiments. The cesium was kept in a glass capsule during the outgasing procedure. After the outgasing procedure the cesium was introduced in the diode by cracking the glass capsule. The glass was removed from the diode. According to the supplier (Merck) the purity of the cesium was 99.98 wt % Cs. After the introduction of the cesium the last measured pressure in the diode was $2\times10^{-8}$ mbar.

The emitter and housing of the diode were electrically grounded. In order to keep the collector and the guard ring at the same electrical potential, two voltage and current

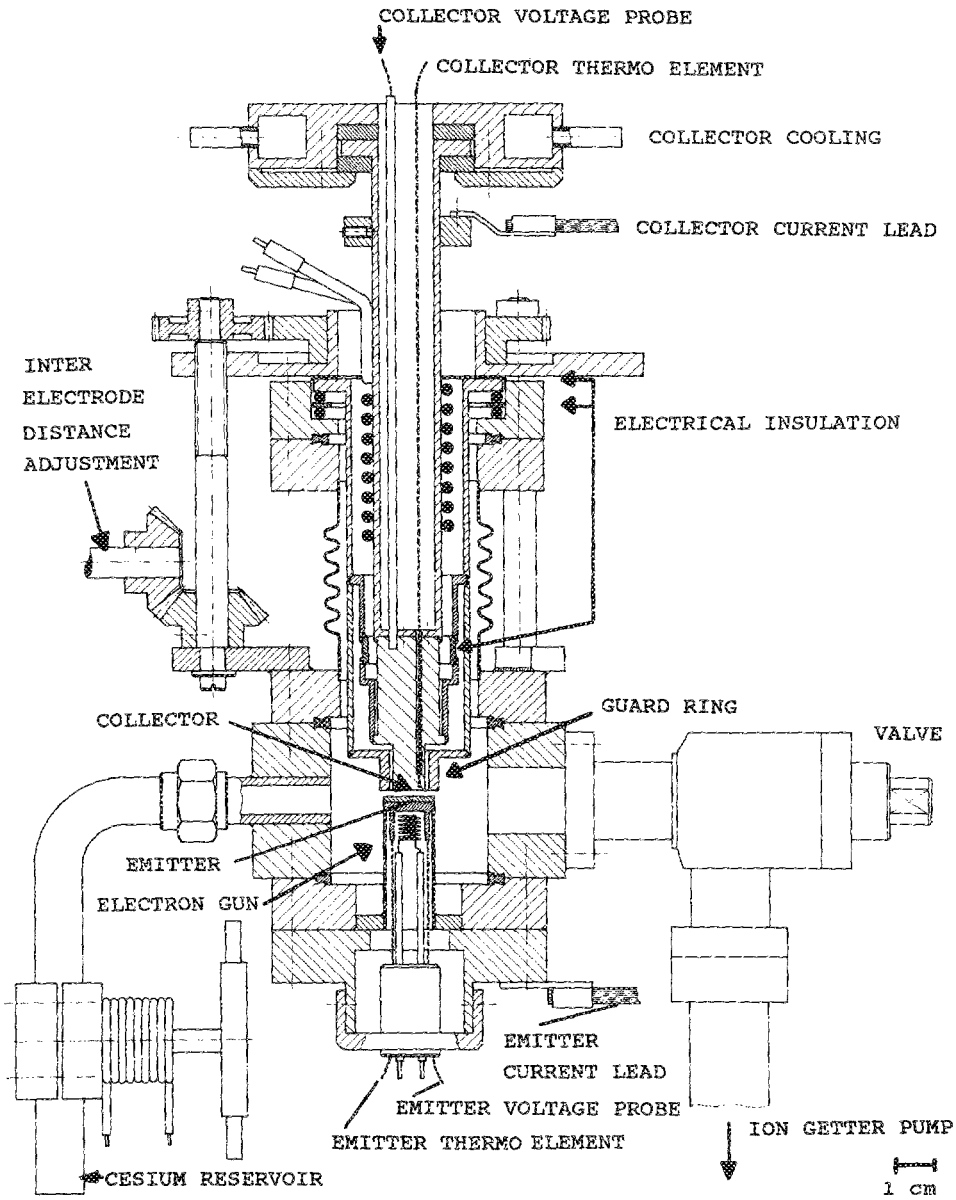


FIG. 3. Schemtic drawing of the research diode.

calibrators (Data Precision, model 8200) were used. The calibrators were computer controlled. In order to measure *I-V* characteristics, the same voltages were applied to collector and guard ring while the collector current was measured.

To avoid the effects of the electrical resistance of the leads when high currents ($>0.1$ A) flow through the diode, we used a four-point method.[5] In order to obtain the *I-V* characteristics at high currents, two Tektronix 577D2 curve tracers with sense connection were used to keep the voltage on the guard ring and the collector the same, while measuring the *I-V* characteristics.

## IV. ELECTRODE MATERIALS

### A. Molybdenum alumina emitter

Samples with various alumina contents were prepared by sintering alumina and molybdenum powders (both with mean particle size of 1 $\mu$m) at 1600 °C in a vacuum of a diffusion pump ($2\times10^{-6}$ mbar). Disks with a diameter of 13 mm and a thickness of 1 mm were machined from the sintered cermets. The samples were ground and polished. A cermet disk was vacuum brazed onto the molybdenum emitter substructure. Mo-42 at.% Ru was used as filler material. The melting temperature of this braze filler material is 1955 °C.

The compositions of the three investigated cermet emitters are given in Fig. 1. In this paper the two emitters with the high alumina content will be described (12.6 and 6.8 at.% Al, which corresponds to 20 and 10 vol % alumina). The features of the pure molybdenum and the 1.8 at.% $Al_2O_3$-Mo emitters are described elsewhere.[5,16] After the sintering process, amounts of $Al_2O_3$ and Mo were determined by x-ray diffraction (XRD). They corresponded to the amounts mixed together before the sinter process. It was found by SEM (EDX) analyses that after the sintering, less than 0.5 at.% Al (the detection limit) had dissolved in the Mo matrix.

As the work function of the emitter is governed by the

TABLE II. Effective bare work function ($\Phi$) of polycrystalline metals and oxides.

| | $\Phi$(eV) | lit. |
|---|---|---|
| Al | 4.27 | [17] |
| Mo | 4.3 | [2] |
| U | 3.53 | [18] |
| $Al_2O_3$ | 4.7 | [19] |
| $UO_2$ | 3.20 | [18] |
| $Mo_3Al$ | 4.0 | (this work) |

outer atom layer, it is of importance to know whether the aluminum segregates to the molybdenum surface. The surface segregation coefficient $s$ [(surface layer concentration)/(bulk concentration)] can be calculated using the equation:

$$s = x^l_{Al}/x^b_{Al} = \exp(-\Delta H_{Al\text{ in }Mo}{}^{surf}/RT), \quad (8)$$

where the values of $\Delta H_{Al\text{ in }Mo}{}^{surf}$ can be deduced from the data given by Miedema.[14] At 1400 °C a surface segregation coefficient $s = 1070$ is found for aluminum in molybdenum, so there is a marked tendency for Al to segregate to the surface. The base pressure in the research diode was $2\times10^{-8}$ mbar. As the water vapor molecules are the most persistent molecules in the diode, it is supposed that the base pressure is the water vapor pressure. The base oxygen partial pressure is then estimated to be $5\times10^{-9}$ mbar. In Sec. II we described that the oxygen partial pressure at the emitter surface is expected to be $2\times10^{-7}$ mbar. Taking into account (1) the surface segration of Al, (2) the equilibrium oxygen partial pressure of the cermet, and (3) the actual residual oxygen partial pressure in the diode, it is possible that, after the outgasing procedure, the total outer surface of the cermet emitter surface consists of $Al_2O_3$. Whether an $Al_2O_3$ layer is formed depends on kinetic aspects, i.e., the evaporation rate of Al and the supply of Al from the bulk of the cermet. The bare work functions of the various clean surfaces of pure metals and oxides are presented in Table II. It is clear from this table that the difference in bare work function of oxygen-free Al and Mo is hard to detect.

After the experiments using a cesium atmosphere in the research diode, the 10 and 20-vol % $Al_2O_3$ cermet emitters were analyzed by x-ray diffraction (XRD): only molybdenum was detected. There was no indication of the presence of $Al_2O_3$ at the emitter surface neither by XRD nor by inspection using a light microscope. The emitter surfaces were analyzed by scanning electron microscopy (SEM) using and EDX detector. A SEM picture of the emitter surface is shown in Fig. 4. No alumina particles were detected at the surface. Figure 4 shows that some molybdenum grains are faceted. The aluminum atom concentration in the molybdenum bulk was found to be less than 0.5 at. %. In some dark spots, increased amounts of Si (17 at. %) and Cs (4 at. %) were found. The emitter surface was investigated with the ESCA technique too. No Al was found on the surface.

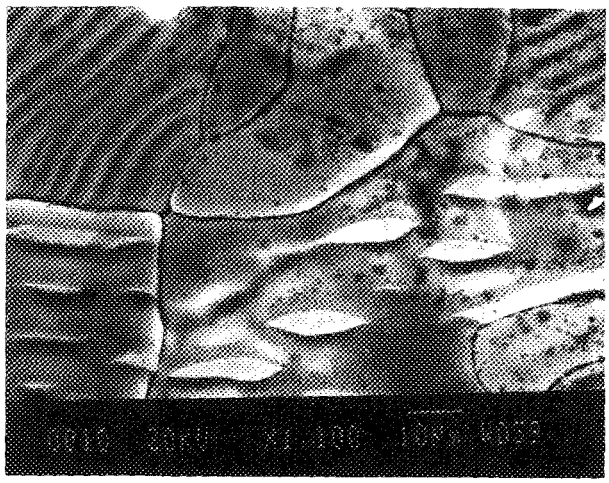

FIG. 4. Secondary electron image (SEI) of the surface of the 10 vol. % alumina molybdenum emitter. Some grains are faceted, i.e., thermally etched. Bar denotes 10 $\mu$m.

A cross section of the emitter was made. Inside the emitter, $Al_2O_3$ grains with a mean diameter of 10 $\mu$m were found (while the original particle size was 1 $\mu$m). In the molybdenum matrix the aluminum concentration was less than 0.5 at. %. A concentration profile over the alumina-molybdenum boundary indicated that also near the boundary ($>2$ $\mu$m) of an alumina particle, the Al concentration in the Mo matrix was low ($<0.5$ at. %).

### B. The molybdenum collector

The collector was machined from an arc cast molybdenum bar. According to the supplier (Amax Inc.) the molybdenum purity was better than 99.97 wt % (ABL2 quality, low carbon). After the experiments performed in the cesium atmosphere of the research diode, the collector surface was covered with a black layer. The surface was analyzed with XRD and was found to consist of $Mo_3Al$ and a few percent $Al_2O_3$. In the SEM (EDX), $Mo_3Al$ was detected too. In a cross section of the collector it was seen that the surface was rough. The mean $Mo_3Al$ layer thickness was found to be 1.5 $\mu$m. We could not detect any $MoO_3$ or additional Mo on the collector surface due to evaporation from the emitter. However, it is hard to discriminate between the Mo of the collector and possible condensed Mo from the emitter.

## V. THE WORK FUNCTION

### A. The work function in vacuum

During the outgasing procedure the electron emission of the emitter was monitored. The base pressure in the diode dropped to $2\times10^{-8}$ mbar and then stabilized while the emitter was at high temperature. A current-voltage ($I$-$V$) characteristic of the 20 vol % $Al_2O_3$-Mo emitter, determined at an interelectrode distance $d = 0.2$ mm is given in Fig. 5. The diode was connected with the ion

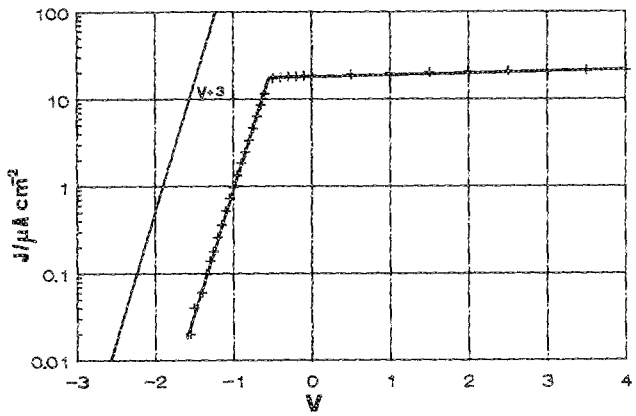


FIG. 5. $I$-$V$ characteristic of a 20 vol % alumina-molybdenum emitter and a molybdenum collector. The emitter and collector temperature were 1436 and 472 °C. The interelectrode distance was 0.2 mm. The base pressure in the diode was $2\times10^{-8}$ mbar. The Boltzmann line ($V+3$) is indicated.

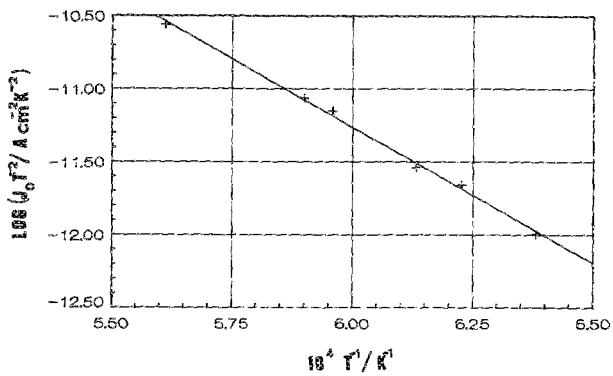


FIG. 6. Richardson plot of the emission current density of a 20 vol % alumina-molybdenum emitter. The interelectrode distance was 0.01 mm. The base pressure in the diode was $2\times10^{-8}$ mbar.

getter pump during this measurement. The saturation current density at zero field ($J_0$) produced by electrons emerging from a homogeneous metal surface is given by the Richardson equation[20]

$$J_0 = A_r T_e^2 \exp(-\Phi/kT_e), \tag{9}$$

where $T_e$ is the emitter temperature in K, $\Phi$ is the work function, $k$ is Boltzmann's constant, and $A_r$ is Richardson's constant. A theoretical value of $A_r$ can be deduced for a uniform surface with a temperature independent work function from statistical thermodynamics of a free electron gas:[20] $A_r = 120$ A cm$^{-2}$ K$^{-2}$. In order to experimentally determine both the work function and Richardson's constant of the emitter, one measures the dependence of the saturation current density ($J_0$) on the temperature. The slope of the plot of $^{10}\log(J_0/T^2)$ vs $1/T$ (Richardson plot) leads to the so-called Richardson work function ($\Phi_r$, also called apparent work function):

$$\Phi_r = -2.3k[d^{10}\log(J_0/T^2)/d(1/T)]. \tag{10}$$

From the intercept of the Richardson plot at $1/T = 0$, the Richardson constant $A_r$ is determined. The Richardson constant determined in this way is called apparent Richardson's constant. Experimentally, Richardson plots are generally found to be straight lines, although the intercept (i.e., the apparent Richardson's constant) is usually not equal to the theoretical constant $A_r$. Work functions calculated from Eq. (9) using the theoretical values $A_r = 120$ A cm$^{-2}$ $T^{-2}$ are called effective work functions ($\Phi_{\text{eff}}$).[1]

The Richardson plot of the 20-vol % $Al_2O_3$-Mo cermet is shown in Fig. 6. A straight line is found. The two apparent Richardson parameters $\Phi_r$ and $A_r$ are obtained from the slope and intercept, respectively: $\Phi_r = 3.70$ eV, $A_r = 0.844$ A cm$^{-2}$ K$^{-2}$. In the investigated range of temperatures both parameters are independent of the temperature. The difference between the theoretically derived and experimentally determined value of Richardson's constant $A_r$ can be attributed to a temperature dependent effective work function. If it is assumed that the Richardson constant $A_r$ is the same both theoretically and experimentally ($A_r = 120$ A cm$^{-2}$ K$^{-2}$) the temperature coefficient of the effective work function can be determined. Inserting Eq. (9) in Eq. (10) while assuming a temperature dependent work function, we obtain:

$$\Phi(T) = \Phi_r + T(d\Phi(T)/dT) \tag{11}$$

showing that $\Phi_r$ would only be the true work function if the temperature dependence of the work function vanished. Assuming that the temperature coefficient $d\Phi/dT$ is constant, substitution of Eq. (11) in Eq. (9) results in:

$$J_0 = 120\ T_e^2 \exp(-\Phi_r/kT)\exp(-k^{-1}d\Phi/dT). \tag{12}$$

Here we use Richardson's constant $A_r = 120$ A cm$^{-2}$ K$^2$, otherwise the temperature coefficient can not be calculated. As stated above, for a 20-vol % $Al_2O_3$-Mo cermet $\Phi_r = 3.70$ eV and $A_r = 120$ $\exp(-k^{-1}d\Phi/dT) = 0.844$, which results in the temperature coefficient for the work function for 20 vol % $Al_2O_3$-Mo cermet of $d\Phi/dT = 4.27\ 10^{-4}$ eV K$^{-1}$. At each temperature the effective work function ($\Phi_{\text{eff}}$) can be calculated using Eq. (11). Of course, the same effective work function at a given temperature can be calculated from the $I$-$V$ characteristic at that temperature using the theoretical value for Richardson constant $A = 120$ A cm$^{-2}$ K$^{-2}$ and Richardson Eq. (9).

From the $I$-$V$ characteristic depicted in Fig. 5 an effective work function of 4.51 eV can be calculated. The effective work functions in Fig. 6 range from 4.36 eV at 1540 K to 4.48 eV at 1820 K. In the retarding field region the current is described[20] by the relation:

$$J = 120T_e^2 \exp[-(\Phi_c - V)/kT_e], \tag{13}$$

where $\Phi_c$ is the work function of the collector. In Fig. 5 the Boltzmann line is depicted, it represents relation (13) for a collector with work function $\Phi_c = 0$ eV. The actual line drawn in Fig. 5 is shifted 3 V in order to bring it within the range of the voltage axis. The Boltzmann line depends only on the emitter temperature. As is seen in Fig. 5 the $I$-$V$ characteristic in the retarding region and the Boltzmann

TABLE III. Effective work functions ($\Phi_e$) of $Al_2O_3$-Mo emitters in vacuum at a temperature of 1700 K. The work functions of the Mo collectors ($\Phi_c$) facing the emitters are indicated too. $c$ is the concentration (in at. %) of the various elements in the emitter.

| Cermet | $c_{Al}$ | $c_{Mo}$ | $c_O$ | $\Phi_e$ (eV) | $\Phi_c$ (eV) |
|---|---|---|---|---|---|
| 20 vol % $Al_2O_3$ | 12.6 | 68.6 | 18.8 | 4.51 | 3.98 |
| 10 vol % $Al_2O_3$ | 6.8 | 83.1 | 10.1 | 4.57 | 3.94 |
| 2.5 vol % $Al_2O_3$ | 1.8 | 95.5 | 2.7 | 4.58 | 4.20[21] |
| 0 vol % $Al_2O_3$ | 0 | 100 | 0 | 4.3 | 4.3[1] |

line are parallel. From Eq. (13) it follows that the slope of the line is determined by the emitter temperature, the slope is $1/(2.3\,kT_e)$. The temperature determined from the slope in Fig. 5 is $T_e = 1791$ K (correlation coefficient 0.9997). This temperature deviates 82 K from the temperature measured with the thermocouple. Although sometimes the $I$-$V$ characteristics were measured over three decades of current, the temperature determined from the slope deviated up to 90 K from the temperature measured with the thermocouple. No systematic deviation in the temperatures could be found. We attribute this deviation to the patch effect resulting from the polycrystallinity of the emitter and the collector.[1] The emitter temperatures indicated in the figures are always the temperatures measured with the thermocouple.

As has been described in Sec. IV B the collector was found to be covered by $Mo_3Al$. The work function of the collector can be obtained from the $I$-$V$ characteristic in the retarding region: the voltage difference between the actual characteristic and the Boltzmann line is the value of the collector work function. From Fig. 5 the collector work function is found to be $\Phi_c = 3.95$ eV. From the deduced emitter and collector work functions (4.51 and 3.95 eV, respectively) a contact potential ($\Phi_c - \Phi_e$) of $-0.56$ V is calculated. Experimentally the contact potential is determined by measuring the voltage at the knee of the $I$-$V$ characteristic. It is demonstrated in Fig. 5 that the same value $V = 0.56$ V is found experimentally.

The effective bare work function of the various alumina-molybdenum cermets in vacuum are given in Table III. The work functions of the 10 and 2.5 vol % $Al_2O_3$ cermets were measured in a diode without a guard ring. However, this should not have any effect since the interelectrode distance was very small (0.01 mm). It is seen from Table III that no clear influence of the amount of alumina on the work function is detected. Taking all data into account we recommend a value of 4.5 eV for the effective bare work function of alumina-molybdenum cermets.

### B. The work function in a cesium atmosphere

In the unignited ion-rich mode, $I$-$V$ characteristics were measured at various emitter temperatures (see Fig. 7). The interelectrode distance is kept small (0.05 mm) during these measurements. In Fig. 7 it is shown that saturation of the emitter emission current occurs within the depicted voltage range. The cesiated effective work function of the cermet emitter is calculated, at each cesium reservoir temperature, from the current density, using Eq. (9). The voltage difference between the Boltzmann line and the actual measured $I$-$V$ characteristic in the retarding range represents the work function of the cesiated collector. From the $I$-$V$ characteristic depicted in Fig. 7 it is calculated that at an emitter temperature of 1200 °C and a cesium reservoir temperature of 200 °C the work function of the emitter $\Phi_e = 2.77$ eV. A collector work function of $\Phi_c = 1.46$ eV is deduced from the voltage difference between the Boltzmann line and the actual $I$-$V$ characteristic. This is corroborated by a value $\Phi_c = 1.48$ eV, which is calculated for the collector work function from the back emission current in the deep retarding range.

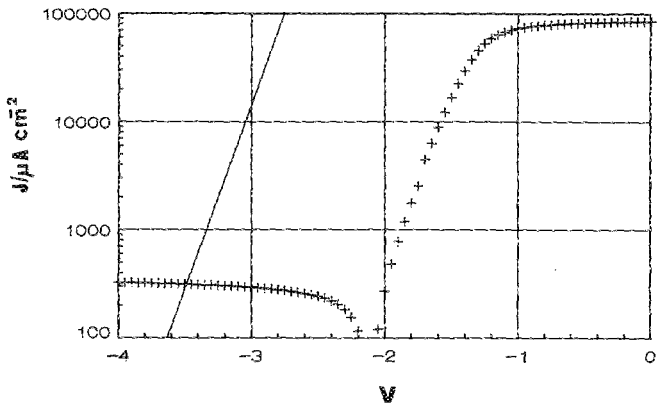


FIG. 7. Electron emission and back emission (sign of the current reversed) of a diode consisting of a 20 vol % alumina emitter and molybdenum collector. Post-morten analysis indicated a $Mo_3Al$ collector surface. The emitter, collector, and cesium reservoir temperature were 1200, 390, and 200 °C, respectively. The interelectrode distance was 0.05 mm. The Boltzmann line is indicated.

It is convenient to plot the work function of cesiated surfaces on a reduced temperature scale. The reduced temperature is the ratio between the electrode temperature and the cesium reservior temperature, both in K. Such a so called, Rasor plot[1] is presented in Fig. 8. Points at the

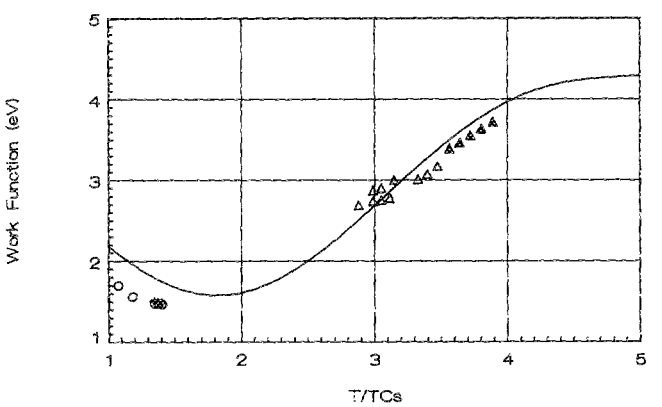


FIG. 8. Rasor plot of the cesiated work functions of the alumina-molybdenum emitter, i.e., △: 20 vol % $Al_2O_3$-Mo, ▲: 10 vol % $Al_2O_3$-Mo. On the surface of the collector $Mo_3Al$ is formed, ○: retarding range measurement, +: back emission measurement.

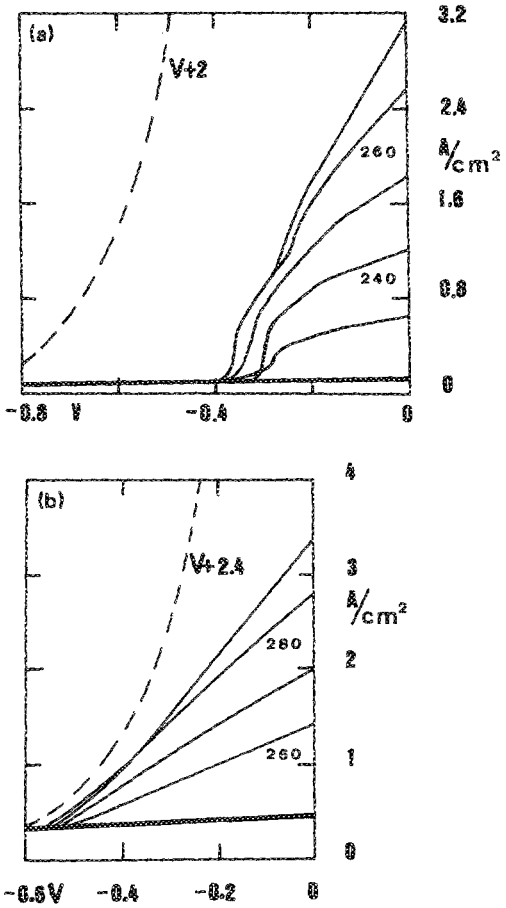


FIG. 9. *I-V* characteristics of the ignited mode of a diode with a 20 vol % $Al_2O_3$-Mo emitter. The interelectrode distance is 0.5 mm. The cesium reservoir temperature is indicated in °C. The dashed line is the Boltzmann line. In (a) the emitter and collector temperatures were 1300 and 550 °C, respectively. In (b) the emitter and collector temperatures were 1400 and 600 °C, respectively.

higher $T/T_{Cs}$ ratios ($T/T_{Cs} \sim 3.5$) are the work functions of the emitter. At lower ratios ($T/T_{Cs} \sim 1.5$) the collector work functions are given. The solid line is the work function of polycrystalline Mo.[1,6] There is an indication that the cermet emitter has a work function which is 0.15 eV lower than that of pure molybdenum. For a practical thermionic energy converter this is a moderate improvement. The cesiated collector facing the cermet emitter has a 0.3 eV lower work function.

## VI. THE IGNITED MODE

### A. Current-voltage characteristics in the ignited mode

At higher cesium reservior temperatures and higher interelectrode distances than used in the measurements discussed in the previous section, the diode ignites and a plasma is created in the interelectrode space. A higher current density is generated by the diode. Various *I-V* characteristics were measured by keeping the emitter temperature, the collector temperature, and the interelectrode distance constant and varying the cesium reservoir temperature. In Fig. 9 two examples are given. The Boltzmann line is again indicated. There are two processes by which the electrons lose energy: (1) entering the collector ($\Phi_c$), and (2) by interactions in the plasma resulting in a plasma voltage drop ($V_d$). These two losses determine the voltage difference between the Boltzmann line and the actually measured *I-V* characteristic. This voltage difference is called the barrier index ($V_b$):

$$V_b = \Phi_c/e + V_d. \tag{14}$$

$V_b$ characterizes the performance of any real thermionic converter: the lower the barrier index, the higher the performance of the converter. The value of the barrier index obtained for the diode with a 20 vol % $Al_2O_3$-Mo emitter is 2.36 V at 1300 °C. The collector work function at these conditions ($T_c/T_{Cs} = 1.51$) is obtained from extrapolation of the data depicted in Fig. 8: $\Phi_c = 1.45$ eV. The plasma drop is then calculated to be $V_d = 0.91$ V.

In Fig. 9(b) it is seen that at an emitter temperature of 1400 °C, the barrier index is still higher, $V_b = 2.5$ V. The plasma drop found at 1400 °C is $V_d = 1.0$ V. The value of the plasma drop obtained with the alumina cermet electrodes is high compared to the value obtained with the usual refractory metal electrodes ($V_d = 0.5$ V).[1]

### B. The electrical power density

The electrical power density (W/cm²) generated by the converter can be calculated from the *I-V* characteristics by simply multiplying the measured current density and the output voltage. The power density is a function of the load voltage. At the conditions depicted in Fig. 9(a) a maximal power density 0.35 W/cm² is found at a load voltage of 0.2 V. The maximal power densities of diodes with various $Al_2O_3$-Mo cermets (20, 10, and 2.5 vol % $Al_2O_3$) were all about the same.

It is impossible to estimate the efficiency of the converter ($\eta$) using the Eq. (2):

$$\eta = P/\{(I/e)[\Phi_c + 2kT_e] + \sigma\varepsilon[T_e^4 - T_c^4]\} \tag{15}$$

where $P$ is the electrical power density, $e$ is the charge of an electron, $\varepsilon$ is the effective thermal emissivity, and $\sigma$ is the Boltzmann coefficient. The efficiency strongly depends on the effective thermal emissivity, which value is the least known. We shall take a value of $\varepsilon = 0.2$ for the effective thermal emissivity.[5] For the calculation of the efficiency, the value of the emitter work function is needed. This value can be calculated by using Eq. (9) and assuming that $J_0$ is two times the current at the knee of the *I-V* characteristic.[1] From the characteristic at $T_{Cs} = 270$ °C ($T_e/T_{Cs} = 2.9$) depicted in Fig. 9(a) a work function of 2.49 eV is calculated. This fits well in the Rasor plot shown in Fig. 7. At 1300 °C emitter temperature and optimized conditions ($T_e = 550$ °C, $T_{Cs} = 270$ °C, $\Phi_e = 2.49$eV, $I = 1.8$ A/cm², $V = 0.2$ V) an efficiency $\eta = 3\%$ is calculated.

The power density increases at higher emitter temperatures.[1] From Fig. 9(b) it can be calculated that the power density is 0.5 W/cm² at 1400 °C.

TABLE IV. Characteristic features of diodes with Mo, $UO_2$-Mo and $Al_2O_3$-Mo emitters. The collector is made of Mo. Collector temperature and cesium reservoir temperature are optimized.

| Emitter material | $T$ (°C) | P (W/cm$^2$) | $\eta$ (%) | $\Phi_e$ (eV) | $\Phi_c$ (eV) | $V_b$ (V) | $V_d$ (V) |
|---|---|---|---|---|---|---|---|
| Mo | 1400 | 4 | 14 | 2.5 | 1.6 | 2.0 | 0.4 |
| $UO_2$-Mo | 1350 | 5 | 15 | 2.35 | 1.3 | 2.0 | 0.7 |
| $Al_2O_3$-Mo | 1300 | 0.4 | 3 | 2.49 | 1.45 | 2.36 | 0.91 |

## VII. DISCUSSION AND CONCLUSIONS

After the outgasing procedure, the bare work function of a freshly polished alumina cermet (both 2.5, 10, and 20 vol % alumina) was found to be 4.5 eV. Experimentally the effective bare work function of the cermets was independent of the relative amounts of oxide and metal in the cermet. All the alumina in the surface region of the cermet emitter had been evaporated. No Al was found to be dissolved in the Mo matrix. The work function of pure Mo in an oxygen free atmosphere is $\Phi = 4.3$ eV, see Table II. As indicated in Sec. II we expected from equilibrium thermodynamic reasoning a work function in vacuum of $\Phi = 4.9$ eV for the Mo cermet at 1400 °C. However, experimentally we found $\Phi = 4.5$ eV. This value corresponds to a lower partial oxygen pressure than corresponds with the three phase equilibrium $Mo/Al_2O_3/MoO_2$. The experimentally determined work function agrees with the estimated residual oxygen pressure in the diode ($5\times10^{-9}$ mbar) at 1400 °C and the data of Greaves and Stickney.[13] Thus the alumina in the bulk of the cermet has no influence on the work function of the cermet.

We assume that the $Al_2O_3$ in the bulk of the cermet emitter decomposes according to reactions (7d). The oxygen diffusion coefficient is given by Bergner[22] to be $D_O = 2\times10^{-10}$ m$^2$ s$^{-1}$ at 1400 °C. Unfortunately we could not find any value for the diffusion coefficient of Al in Mo in the literature. Because of the low oxygen concentration in the Mo matrix ($c_O = 10^{-2}$ mol m$^{-3}$), the oxygen permeability ($c_O D_O$) of the Mo matrix is the rate limiting step for the $Al_2O_3$ decomposition in the bulk of the emitter, $c_O D_O = 2\times10^{-12}$ mol m$^{-1}$ s$^{-1}$.

The Al permeability of the Mo matrix is supposed to be that high, and that all free aluminum diffuses to the surface. This diffusion is enhanced by surface segregation. Due to the high vapor pressure of Al($g$) at the surface of the cermet ($3\times10^{-7}$ mbar at 1400 °C) all Al evaporates. The aluminum condenses on the collector to form $Mo_3Al$. The collector is an Al sink. As a result of these kinetic aspects, no Al solubility in the Mo matrix can be found experimentally. The Al concentration at the alumina molybdenum interface decreases within 2 $\mu$m to below 0.5 at. %.

In the presence of Cs the partial oxygen pressure in the diode is determined by the getter function of the liquid Cs in the cesium reservoir ($T_{Cs} = 280$ °C). 28 at. % O is soluble in liquid Cs.[7] Until the first amounts of $Cs_2O$ are formed the partial oxygen pressure is lower than $10^{-19}$ mbar. Thus the partial oxygen pressure at the emitter surface is inclined to be even lower than in the vacuum diode. Al will evaporate and condense on the collector. The supply of Al from the bulk of the cermet is too low to cause any influence of Al on the work function of the cermet surface.

For the cesiated work functions of the cermet emitters we found a value 0.15 eV lower than measured for pure molybdenum. According to Rasor's model,[6,23] this lower cesiated work function is consistent with the 0.2 eV higher bare work function. The cesiated work function of the Mo-$UO_2$ emitter[4] was found to be 0.5 eV lower than the work function of cesiated Mo, see Sec. I. This is the main reason for the high power density of the diode with the Mo-$UO_2$ emitter. We want to stress that the 0.5-eV lower cesiated work function of the cesiated Mo-$UO_2$ emitter agrees with the 0.6-eV higher bare work function expected for Mo cermet electrodes.

The power density of the diodes with the $Al_2O_3$-Mo emitters was rather low compared with both pure Mo and $UO_2$-Mo emitters, as shown in Table IV. However, the published power densities of converters with "pure" Mo electrodes differ by a factor four.[5] The most carefully outgased diodes do not have the highest power density. Of course, other impurities than oxygen are important too, e.g., carbon and sulfur.[24]

As a real converter has to sustain high heat fluxes and high current fluxes it is difficult to design a converter where electrodes, both emitter and collector can be flashed to the high temperature of 2100 K, in order to desorb all contaminations from the electrodes, and even when such a design is realized, it will be difficult to make such a clean diode that the electrodes, both emitter and collector, remain uncontaminated during long periods of time (2000 h).

Comparing the data collected in Table IV we conclude that the main difference between the $Al_2O_3$-Mo emitter and the $UO_2$-Mo emitter is the high barrier index $V_b$. The high barrier index of the $Al_2O_3$-Mo emitter diode stems from the high plasma drop $V_d$ in this diode. Besides the voltage drop over the plasma arc, the "nonideal surface aspects"[21] also are included in the plasma drop. The plasma drop in the $UO_2$-Mo diode was low because the emitter work function had its optimal value (2.4 eV) at a higher reduced temperature, i.e., the optimal cesiated work function of Mo-$UO_2$ was reached at a lower cesium reservior temperature than in the case of Mo or Mo-$Al_2O_3$ emitters. An additional reason for the high plasma drop in the diode with the Mo-$Al_2O_3$ emitter may be that the resistance of the Cs-plasma increases as a result of the small amounts of Al in the interelectrode space.

From thermodynamic analysis it is clear that the par-

tial oxygen pressure of a Mo-oxide cermet can be influenced by the amount of metal (e.g., Al or U) that is dissolved in the Mo matrix. In this respect it is of interest that Henne indicated that "an over-stoichiometrical content of oxygen in the uranium oxide"[4] gives the best result. The $UO_2$-Mo electrodes need further investigation. We should know whether the high power density is reproducible and whether it is caused by residual oxygen or by the oxygen from $UO_2$. Attention should also be payed to the U concentration in the Mo matrix and the segregation of U in Mo.

In our opinion the influence of the residual oxygen pressure is of more importance to the characteristics of a converter than the alumina of a cermet emitter. A cermet emitter will only have a beneficial effect on the power density of a diode, if the metal component of the oxide diffuses so slowly in the Mo matrix, that it controls the oxygen flux in the Mo matrix. For that reason cermets of Mo with $UO_2$ or $Ta_2O_5$ may be better electrode materials.


[1] G. N. Hatsopoulos and E. P. Gyftopoulos, *Thermionic Energy Conversion* (MIT, Cambridge, MA, 1979), Vols. I and II.

[2] F. G. Baksht, G. A. Dyuzhev, and A. M. Martsinovskiy, *Thermionic Converters and Low Temperature Plasma*, English ed., edited by L. K. Hansen, DOE tr1.1 (Technical Information Center, Springfield, VA, 1978).

[3] G. H. M. Gubbels, L. R. Wolff, and R. Metselaar, Appl. Surf. Sci. **40**, 193 (1989); and **40**, 201 (1989).

[4] R. Henne and W. Weber, in *Proceedings of the Thermionic Energy Conversion Specialist Conference*, edited by B. Devin (Eindhoven University of Technology, Eindhoven, Netherlands, 1975), p. 31.

[5] G. H. M. Gubbels, L. R. Wolff, and R. Metselaar, J. Appl. Phys. **64**, 1508 (1988).

[6] N. S. Rasor and C. Warner, J. Appl. Phys. **35**, 2589 (1964).

[7] Binary Alloy Phase Diagrams, edited by T. B. Masalski, American Society of Metals (1986).

[8] *CRC Handbook of Chemistry and Physics*, edited by R. C. Weast (CRC, Boca Raton, FL, 1979).

[9] I. Shilo and H. F. Franzen, J. Electrochem. Soc. **129**, 2615 (1982).

[10] G. H. M. Gubbels, Mater. Sci. Eng. (to be published).

[11] K. K. Schulze, H. A. Jehn, and G. Horz, J. Metals **40**, 25 (1988).

[12] Gmelin Handbuch der Anorganische Chemie, Wolfram, Molybdenum, edited by H. Katscher and K. Swars (Springer, Berlin, 1978).

[13] W. Greaves and R. E. Stickney, Surf. Sci. **11**, 395 (1968).

[14] A. R. Miedema and A. K. Niessen, *Cohesion in Metals* (North-Holland, Amsterdam, 1989).

[15] *Gmelin Handbuch der Anorganische Chemie, Uran*, edited by R. Keim, (Springer, Berlin, 1977).

[16] G. H. M. Gubbels and L. R. Wolff, in *Proceedings of the 23rd Intersociety Energy Conversion Engineering Conference*, edited by D. Yogi Goswami (The American Society of Mechanical Engineers, New York, 1988), Vol. 1, p. 617.

[17] J. Holzl and F. K. Schulte, in *Springer Tracts in Modern Physics*, edited by G. Hohler (Springer, Berlin, 1979), Vol. 85.

[18] W. McLean and H. L. Chen, J. Appl. Phys. **15**, 4679 (1985).

[19] V. Fomenko, *Emission Properties of Materials* (NTIS, Springfield, VI, 1972).

[20] G. A. Haas and R. E. Thomas, in *Techniques of Metals Research, Vol. VI, Measurement of Physical Properties*, edited by E. Rassaglia, (Wiley, New York, 1972), p. 91; C. Herring and M. H. Nichols, Rev. Mod. Phys. **21**, 185 (1949).

[21] G. H. M. Gubbels, *The Thermionic Work Function of a Molybdenum (1 wt %) Alumina Electrode, Internal Report* (Eindhoven University of Technology, Eindhoven, Netherlands, 1988).

[22] D. Bergner, in *Diffusion and Defect Monograph Series No. 7*, edited by F. J. Kedves and D. L. Beke (Trans Tech SA, Switzerland, 1983), p. 223.

[23] N. S. Rasor, Appl. At. Coll. Phys. **5**, 169 (1982).

[24] R. G. Musket, Appl. Surf. Sci. **10**, 143 (1982).